Desalination and Water Treatment
www.deswater.com
doi: 10.1080/19443994.2014.926835

55 (2015) 1467–1479
July

Taylor & Francis
Taylor & Francis Group

Simulation of mercury bioremediation from aqueous solutions using artificial neural network, adaptive neuro-fuzzy inference system, and response surface methodology

Seyed Ali Jafari[a], Dariush Jafari[b,*]

[a]*Department of Biotechnology, Persian Gulf Research Institute, Persian Gulf University, 75169 Bushehr, Iran, Tel. +98 771 4546518; email: sajafari.pgrsc@yahoo.com*
[b]*Department of Chemical Engineering, Bushehr Branch, Islamic Azad University, Bushehr, Iran, Tel. +98 771 4540422; email: dariush.jafari@yahoo.com*

Received 29 November 2013; Accepted 18 May 2014

ABSTRACT

In the present study, an indigenous strain of *Vibrio parahaemolyticus* PG02 has been used for mercury elimination from aqueous solutions. A test was performed for evaluating minimum inhibitory concentration of $HgCl_2$ on the growth of PG02, which revealed that it tolerated up to 45 mg l^{-1} Hg^{2+}. When the bacteria initially exposed to 5 mg l^{-1} mercury in the medium, during 40 h of incubation, it could remove more than 87% of the initial mercury while this value decreased to 79% when initially exposed to 10 mg l^{-1} mercury. The intelligent modeling systems including artificial neural network (ANN) and adaptive neuro-fuzzy inference system were proposed due to the complexity and nonlinearity of such process. They were constructed on the experimental data which obtained using central composite design under response surface methodology. The results of fitting the experimental data revealed an excellent fitting by all of three examined models. This suggests reliable models for prediction of the current process performance. However, verification experiments, which were conducted to confirm the precision of proposed models, introduced the ANN model as the best for mercury removal from aqueous solution by bacterial strain of *Vibrio parahaemolyticus* PG02.

Keywords: Mercury; Bioremediation; Modeling; RSM; ANN; ANFIS

1. Introduction

Traditional physico-chemical techniques that have been used to remove heavy metal contaminations from water or wastewater sources have not been successful enough due to the high costs, production of hazardous by-products, and low efficiencies. Such specifications are related to operations such as precipitation, adsorption, ion exchange, coagulation, flocculation, reverse osmosis, complexation, and electrochemical operations [1–3]. In recent years, microbial bioremediation has been introduced as an affordable technique for heavy metals removal from environment because of low cost, environmentally friendly, and good efficiency especially at low metal concentrations [2,4,5]. The elimination of mercury, as one of the most dangerous elements for human health, has received more attention than other heavy metals [3,5,6].

*Corresponding author.

Complete bacterial detoxification of mercury is obtained by reduction of Hg^{2+} to Hg^0, using mercury reductase enzymes and diffusional loss of Hg^0 from the cell [7]. Many investigations in this field suggest that there are many microorganisms as biomasses of bacteria, algae, and fungi, which exhibit interesting capacities for mercury removal from water or wastewater [1,8–14].

An efficient process modeling helps to optimize the process performance while prevents extra expensive experiments and waste of time. When a system is complex to interpret and also the detailed information is not available, or the process have a nonlinear time variable behavior, the results of analytical modeling using knowledge-based approaches may not be convincing. For such complex processes, the simplifying assumptions may limit the accuracy of proposed models. However, for some processes, it is possible to obtain an analytical model with a sufficient accuracy [15]. These ambiguities have made strong tendencies on modeling based on direct use of empirical data using intelligent systems such as artificial neural network (ANN), adaptive neuro-fuzzy inference systems (ANFIS), and fuzzy logic (FL) [16,17]. The mentioned predictive models provide results with excellent correlations and can be used to model the nonlinear relations over a wide range of input variables [15].

The capability of these modeling methods has been approved before in economics, robotic, material science, chemistry and chemical industry, environment, new energy sources, oil industry, etc. [18–20]. In this contribution, there has been a wide range of chemical engineering publications such as studies on catalyst behavior [17], normal cutting forces [16], water treatment [21–24], thermosyphon thermal performance [25], crude oil viscosity [19,20], wind generator optimized performance [19], cavity thermal performance [26], and membrane processes [18].

The accuracy of such models may be more impressive when the operating parameters of process are optimized by a technique such as response surface methodology (RSM) [15]. Rahmanian et al. used RSM in order to optimize the lead removal from aqueous solutions using micellar-enhanced ultrafiltration followed by FL model to simulate the process [23]. Xie et al. proposed a FL model and RSM approach in an effort to reduce the number of experiments [15]. In another study, Kim and Rhee proposed a FL controller with RSM [27]. Ravikumar et al. used RSM and ANN approaches for the optimization and modeling of decolorization process of distillery spent wash by *Phormidium valderianum* [28]. Mohamed et al. employed RSM to study the effect of medium variables on biomass concentration of microalgae *Tetraselmis* sp. and lipid yield. An ANN approach was then employed for predicting a composition that would result in maximum lipid productivity by the studied strain [29].

In this study, the performance of mercury bioremediation process using an indigenous resistant strain of *Vibrio parahaemolyticus* PG02 was simulated using ANN and ANFIS approaches. An experimental design strategy using CCD was conducted in order to evaluate the effect of operative parameters such as pH, temperature, and initial mercury concentration on the mercury removal percentage as well as comparing the precision of proposed model by RSM with ANN and ANFIS models. A verification study was also conducted to assess the precision of the proposed models.

2. Theory

2.1. Response surface methodology

RSM is a collection of mathematical and statistical techniques that has been applied to optimize and model in numerous chemical and biochemical processes in the last few years [30–32]. It can simultaneously represent the effects of main factors and their interactions on desired response and also determines the optimum values [33]. The required number of experiments that can be designed by RSM are much less than a full experimental design at the same level [23].

The relationship between response and independent factors usually is described by an empirical second-order polynomial model as is presented in Eq. (1) [30,31,33]:

$$Y = \beta_0 + \sum_{i=1}^{k} \beta_i x_i + \sum_{i=1}^{k} \beta_{ii} x_i^2 + \sum_{i=1}^{k-1} \sum_{j=2}^{k} \beta_{ij} x_i x_j \quad (1)$$

where x_i, x_i^2, and $x_i x_j$ are the linear or main, squared, and the interaction effects of independent factors, respectively; and β_0, β_i, β_{ii}, and β_{ij} are the constant, linear, squared, and the interaction effect coefficients, respectively. The accuracy of fit of the proposed model is interpreted by the coefficient of determinations, R^2 and adjusted R^2 [29].

2.2. Artificial neural network

Neural networks (NNs) which are inspired by biological systems are computer algorithms comprised of elements called neurons. They are applied for information processing purposes. Actually, they are neurocomputers which possess parallel distributed processors [26]. Neurons are the main elements of NNs which are connected to the networks by a set of

connections called assigned weights. The performance of a network is strongly dependent on weights values. The neurons are organized in input, output, and the hidden layers. A neural network performs the modeling affair in a way that receives the input, sums them with their weights and adds a bias to the result of summation, then sends the results as an argument to the transfer function.

There are several types of NNs, where multilayer perception (MLP) is the most common one [34]. The MLP network has one input layer, one output layer, and usually one hidden layer. The number of input and output variables of the network depends on the type of process [20]. As mentioned in majority of cases, a network with one hidden layer leads to satisfactory results. Therefore, the number of hidden layer is the considered one in this paper. Each neuron in a layer is usually connected to the neurons of the latter one.

The network training is done by assigning a pattern to the input pattern, after that the results of activation level calculation are propagated forward toward the output layer. Calculation units sum the inputs and utilize a function to calculate the output. Finally, the output of the network is achieved in the output layer. The improvement of network convergence is done by the addition of a constant term by the bias units of the input and hidden layers to the weighted sum. When the network outputs are compared with the target values, the errors of hidden units are determined, and then their weights are manipulated to minimize the error. This procedure is shown in Fig. 1. Generally, it can be claimed that the reduction of global error is the consequent of weight and bias adjustment using training algorithms.

The neuron k can be expressed mathematically using Eqs. (2) and (3):

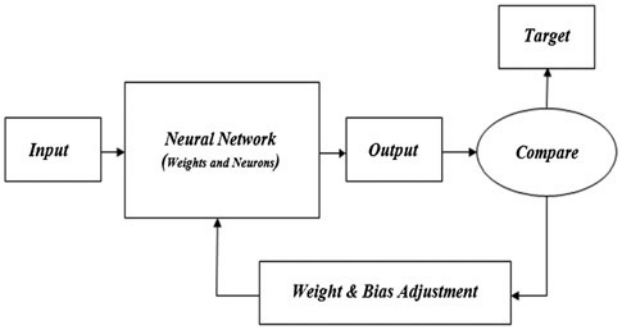

Fig. 1. A schematics of ANN model and weight and bias adjustment.

$$u_k = \sum_{j=1}^{m} w_{kj} x_j \tag{2}$$

$$y_k = \varphi(u_k + b_k) \tag{3}$$

where x_j is the input signal, w_{kj} is the neuron's weight, u_k is the linear combiner output due to input signals, b_k is its bias, φ is the activation function, and y_k is the output signal of neuron.

MLP neural network is used in the current study, where it is trained by the Levenberg–Marquardt (LM) algorithm. The transfer functions of hidden and output layers are linear. The current training algorithm has provided the lowest error value; consequently, the optimal number of hidden layer neurons has been achieved. The operating parameters are pH of the medium, temperature, and initial Hg^{+2} concentration, so the input layer of the network has three neurons. The output is Hg^{+2} removal percentage, which results in one neuron in the output layer. The number of hidden layer neurons is achieved by the training of several networks with different number of hidden layer neurons and the comparison between the results of predictions for the desired output. The number of hidden layer's neurons is equal to 20 in this network. The adequacy criterion for the optimized number of neurons is determined by the calculation of mean squared error (MSE) between the network output and the training data. MSE is calculated by the following equation:

$$\mathrm{MSE} = \frac{\sum_{i=1}^{n} (Y_{\mathrm{Model},i} - Y_{\mathrm{exp},i})^2}{n} \tag{4}$$

2.3. Adaptive neuro-fuzzy inference system

The main purpose of a computer software which is based on artificial intelligence is the achievement of a set of input–output relationships which describe specific processes [35]. The word specific implies processes which have difficulties in mathematical modeling such as nonlinear, adaptive learning, and real time processes.

The learning ability of NNs combined with fuzzy modeling has created the ANFIS system which is actually a fuzzy inference in the form of adaptive networks [36]. In other words, ANFIS is a hybrid neuro-fuzzy system which utilizes the appropriate features of ANN and fuzzy models while corrects their inappropriate properties [37]. ANFIS has a FL context and uses ANN to determine the shape of rule extraction and

membership functions (MFs) [38]. It can be said that ANFIS is the combination of low-level calculation of ANN along with the high reasoning ability of a FL system [19].

In the modeling of nonlinear systems based on ANFIS, the input space is divided into many local regions. A simple local is developed for each one based on linear functions or adjustable coefficients, then ANFIS uses the MFs to divide dimensions of each input. Several local regions can be activated simultaneously, while the input space is covered by the overlapping MFs. The MFs and the ANFIS layers play an important role in approximation ability of ANFIS model [26].

ANFIS comprises two parts. The first part is antecedent and the second is conclusion part. Fuzzy rules relate these two parts.

A common fuzzy if-then rule is as the following equation:

Rule 1:

If x_1 is A_1 and x_2 is B_1 and etc.; then $f_1 = p_1x_1 + q_1x_2 + \cdots + r_1$;

Rule 2:

If x_2 is A_2 and x_2 is B_2 and etc.; then $f_1 = p_2x_1 + q_2x_2 + \cdots + r_2$

where A_i, B_i and, f_i are the fuzzy and output sets. p_i, q_i, and r_i are the design variables which are determined during the learning [39].

ANFIS modeling is done in five layers as illustrated in Fig. 2 [36].

The nodes of the first layer are adaptive nodes with the following function (Eq. (5)):

$$\mu_{Ai}(x) = e^{-\left(\frac{x-x^*}{\sigma^2}\right)} \tag{5}$$

where x^* and σ^* are premise parameters which are adapted by a hybrid algorithm and x is the input variable. In the second layer, the firing strength of each rule is determined by quantifying the extent of each rule's input data. The output of a layer is the algebraic product of input signals:

$$O_{2,i}(x) = \omega_i = \mu_{Ai}(x_1) * \ldots * \mu_{Ci}(x_n) \tag{6}$$

The normalization is performed in the third layer. It is done by the calculation of ratio of ith, rule's firing strength to the summation result of all rule's firing strength, it is calculated by each node as the following:

$$O_{3,i}(x) = \bar{\omega}_l = \frac{\omega_i}{(\omega_i + \ldots + \omega_n)} \tag{7}$$

The output of each node is calculated in the fourth layer as following equation:

$$O_{4,i} = \sum \bar{\omega}_i f_i \tag{8}$$

The total output is determined as the summation of all input signals in the fifth layer. The calculation of wave height in layer five is done using the following equation [19,24,40]:

$$O_{5,i} = \frac{\sum_{i=1}^{n} \omega_i f_i}{\sum_{i=1}^{n} \omega_i} \tag{9}$$

It is obvious that the first and the fourth layers are adaptive. C_i and O_i are premise parameters of input fuzzy MFs in layer 1 [39]. As mentioned, the fifth layer gives the total output as the sum of all input signals.

Several ANFIS models have been applied to perform the modeling using MATLAB software. Additionally, the coverage threshold is equal to 0.045. It is worth noting that the Gaussian MFs have been used in this work.

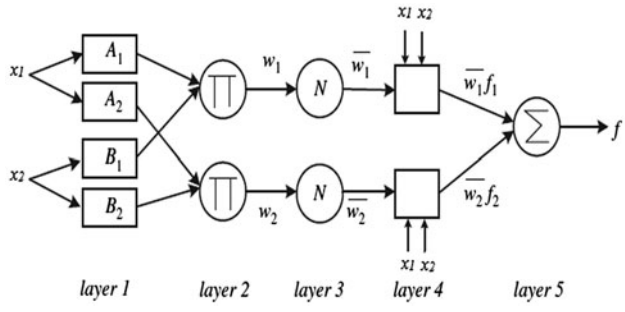

Fig. 2. The structure of ANFIS model.

3. Material and methods

3.1. Microorganism

The bacterial strain which was used in the present work had been previously isolated from contaminated sediments of Bushehr (Iran) coast and identified as *Vibrio parahaemolyticus* PG02 [41]. This strain has been deposited in NCBI GenBank under accession number of KC990033. Pure colonies were maintained on Tryptic Soy Agar plates at 4°C.

3.2. Minimum inhibitory concentration test

In order to study the maximum bacterial resistance to mercury, the minimum inhibitory concentration

(MIC) test was conducted. It is known as the lowest concentration of Hg^{2+} that completely prevents the growth of microorganism [42]. In order to calculate the MIC, 1 ml aliquots of overnight cultures were inoculated in 99 ml of Tryptic Soy Broth (TSB) and 5 ml was distributed in 20 test tubes. Various concentrations of Hg^{2+} were added (from 5 to 100 mg l^{-1}). Tubes were then incubated in a shaker incubator at 160 rpm and 35˚C for 24 h [41]. The optical density of each culture was detected at a wavelength of 560 nm, using a UV–visible spectrophotometer (PerkinElmer, Lambda 25, USA) [13]. The Control samples containing culture medium and mercuric chloride, without bacteria, were also assessed simultaneously with the main tests. It is worth noting that the experiments were carried out in duplicate.

3.3. The rate of mercury bioremediation by strain PG02

The toxicity of heavy metals especially mercury has deathlike effects on living cells, and this will appear as declining specific growth rate of microorganisms as well as premature death [43,44]. So it can be acclaimed that the heavy metal bioremediation process will be performed as long as the microorganisms are metabolically active. Therefore, in order to investigate the approximate time to accomplish the mercury bioremediation process, which means after that there is no significant change in mercury concentration in the medium, some experiments were conducted to monitor the mercury concentration in the culture medium over time. Therefore, three 500 ml flasks containing 250 ml TSB with the initial concentrations of 5, 10, and 40 mg l^{-1} Hg^{2+} were inoculated with 12.5 ml (5%) of overnight culture and incubated at 160 rpm, 35˚C, and pH value of (8.1 ± 0.1) in a conventional shaker incubator. The bacterial-free mediums containing defined mercury concentrations were incubated as control runs. Sampling was done in certain time intervals followed by centrifugation (7,000 × g for 20 min) in order to analyze the residual mercury in supernatant by flameless Atomic Absorption Spectrophotometer (PG Instruments AAS 500, England). All of the experiments were carried out in triplicate and confidence intervals of 95% were calculated for the averages.

3.4. Design of experiment using RSM

The central composite design (CCD) under RSM was applied using MINITAB software (version 14.1) as an experimental design strategy and modeling the mercury removal process. The ANN and ANFIS modeling approaches were constructed on the experimental data obtained by this design strategy. Initial pH of medium (levels of 2, 3, 5, 7, and 8), temperature (levels of 20, 25, 35, 45, and 50˚C), and initial Hg^{2+} concentration (levels of 5, 10, 20, 30, and 35 mg l^{-1}) were considered as three independent factors affecting the mercury removal percentage, as response. Forty experiments were employed with two replicates in 100 ml flasks containing 50 ml TSB culture medium under specified conditions to evaluate the effect of three independent factors on mercury removal by PG02. The runs were incubated at 160 rpm in a conventional shaker incubator. The samples were withdrawn after 40 h of incubation followed by centrifugation (7,000 × g for 20 min) and analyzing the supernatant by AAS. The removal percentage (response) was calculated according to Eq. (10):

$$\%\,\text{removal} = \frac{(C_i - C_t)}{C_i} \times 100 \tag{10}$$

where C_i and C_t are the initial and the residual mercury concentrations (mg l^{-1}) at time t, respectively.

4. Results and discussion

4.1. The rate of mercury bioremediation

The experiments have showed that PG02 can resist up to 45 mg l^{-1} Hg^{2+}. It is significantly more resistant in comparison with some other reported *Vibrio* species with MIC values of 2.71 and 12–16 mg l^{-1} Hg^{2+} [45,46]. However, it is weaker than *Pseudomonas* sp. with MIC = 100 mg l^{-1} Hg^{2+} [47]. Plasmid-containing feature of *Vibrio parahaemolyticus* makes it resistant against high concentrations of pollutants [45]. Therefore, the bioremediation studies by PG02 were conducted below 45 mg l^{-1} Hg^{2+} concentrations.

Tracing the mercury concentration in the culture medium under adjusted conditions (35˚C, 160 rpm and pH of 8.1 ± 0.1) revealed that increasing the initial mercury concentration decreased the rate of bioremediation (Fig. 3). As was previously claimed, it is due to the bacterial deactivation. In Fig. 3, it can also be seen that when the initial mercury concentration was 5 mg l^{-1} in the medium, the concentration decreased rapidly during the first 20 h of incubation and reaches to 1 mg l^{-1} (79% mercury removal). It occurred during the logarithmic phase of growth. However, during the next 20 h, when the bacteria placed in the stationary phase, fewer changes were observed in mercury concentration such that it only decreased to 0.6 mg l^{-1} (87% mercury removal). After that, no significant changes were observed in mercury concentration in

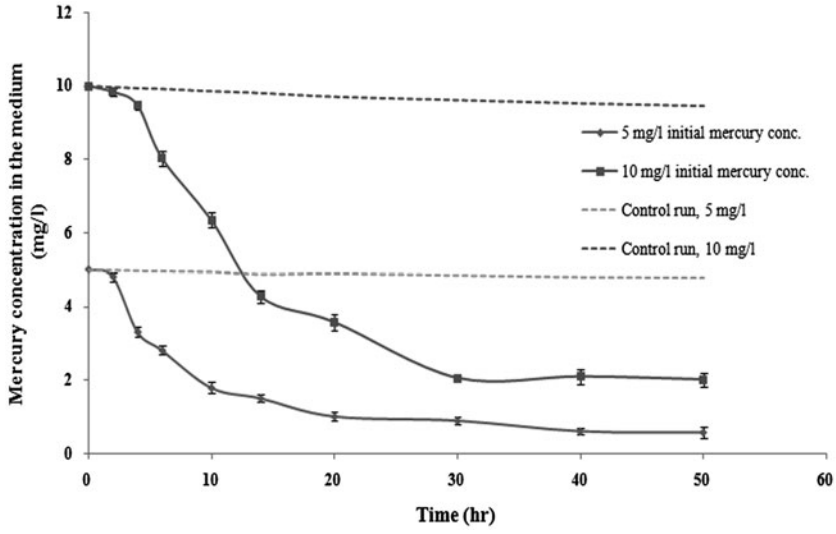

Fig. 3. Decrease in mercury concentration by *Vibrio parahaemolyticus* PG02 over time when the initial mercury concentration was (♦) 5 mg l^{-1} and (■) 10 mg l^{-1} along with the control runs (–), Temperature of 35°C, 160 rpm and pH 8.1 ± 0.1.

the medium and the bioremediation process gradually stopped.

The same trend was observed when the initial mercury concentration was adjusted to 10 mg l^{-1} in the medium (Fig. 3). However, the whole decreasing phase of mercury concentration in the medium occurred during the first 30 h of incubation (79% mercury removal) and beyond this time there were not any significant changes in the mercury removal. It means that the increase of the mercury concentration time required to carry out the bioremediation process is decreased. The diagram of 40 mg l^{-1} mercury concentration was not depicted since no significant reduction was observed in its concentration during the incubation time and the rate of bioremediation was almost negligible (less than 10% mercury removal). It was previously confirmed by Schmitz et al. [44] that the specific growth rate of *V. fischeri* was significantly decreased in the presence of Chromium, Manganese, and selenium. Kafilzadeh and Mirzaei also demonstrated that *Klebsiella* and *Pseudomonas* almost became disabled in the presence of 20 mg l^{-1} mercury in the medium [43].

According to Fig. 3, a slight depletion was observed in mercury concentrations during the control runs which were indicated by dash lines. It is presumably due to the sorption of mercury ions by the glass surface of the flask. As it was approved by Stas' et al. [48], glass can adsorb cations. In the present research, less than 5% of initial mercury concentrations were disappeared in control runs, which can be ignored.

By these findings, the sampling was done in the following RSM experiments after 40 h of incubation.

4.2. Prediction results of RSM

Samples were withdrawn from all of the 40 experiments that were designed by RSM after 40 h of incubation in order to measure their residual mercury contents by AAS. After analyzing the obtained experimental data by MINITAB, a modified polynomial quadratic model was achieved as a function of studied factors which was indicated in Eq. (11):

$$\begin{aligned} Y\,(\text{Mercury Removal }\%) = {} & 17.2162 + 8.0917 \times \text{pH} \\ & + 2.6818 \times \text{Temp} - 1.4346 \\ & \times \text{Hg Conc.} - 0.6735 \times \text{pH}^2 \\ & - 0.0399 \times \text{Temp}^2 - 0.0307 \\ & \times \text{Hg Conc.}^2 \\ & + 0.0384\,\text{pH.Temp} \\ & + 0.0087\ \text{Temp.Hg Conc.} \end{aligned} \tag{11}$$

As it can be seen from Eq. (11), the mathematical signs of the main effects indicate that pH and temperature have positive influence on the response while initial Hg concentration has a negative influence [33]. In addition, the larger coefficient of pH (8.0917) compared with the other main effects represents the greater impact of this factor on the response, *Y*. The high values of $R^2 = 0.999$ and adjusted $R^2 = 0.998$ indicate an

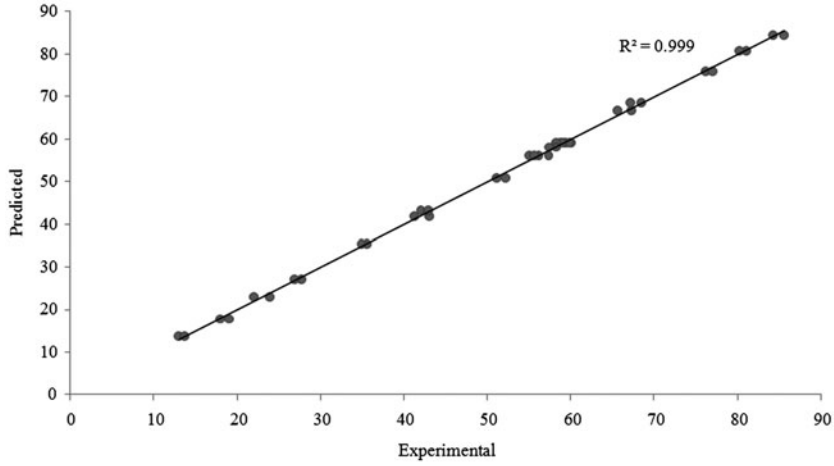

Fig. 4. Comparison of experimental data and predicted values by RSM for mercury removal by PG02.

excellent agreement between the experimental and the predicted values as illustrated in Fig. 4.

Fitting evaluation based on R^2_{adj} is more accurate than by R^2 [29]. However, the statistical significance of the model should also be assessed by *P*-values of the model and lack-of-fit terms. The former should be significant with value less than 0.05 and the latter should be insignificant with value more than 0.05 [29,49]. Here, both of these terms were satisfactorily accepted by the values of 0.000 and 0.172, respectively. Therefore, the modeling by RSM can be considered reliable for prediction of mercury removal by studied strain, PG02. Verification experiments were also performed to assess the precision of the model.

It was found that increasing the pH value up to 7.2 increased the mercury removal sharply, while the response decreased slowly at higher pH values. The temperature also showed to have a similar effect. The value of 37.5˚C exerted the most significant effect on mercury removal among the considered values. Such an effect can be interpreted as the stimulation of bacterial activity and cell division by environmental factors such as pH and temperature [50]. However, the increase in the pH leads to the deprotonation of functional groups on the cell surface and this, in turn, increases the attractive forces between the cell wall and Hg^{2+} ions [5]. On the other hand, the bioaccumulation is a temperature-dependent mechanism [51,52], but excessive temperature destroys or deactivates the cells [50]. The initial Hg^{2+} concentration exerted a reverse effect on the mercury removal percentage by PG02. Increasing the initial mercury concentration from 5 to 30 mg l^{-1} decreased the removal percentage from 90 to 33%. As was previously discussed, high concentrations of mercury decreased the bacterial growth and consequently the mercury bioremediation.

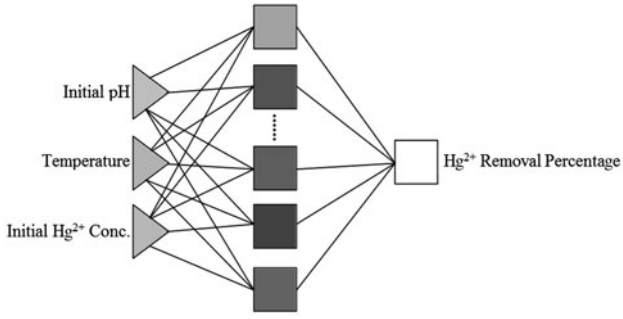

Fig. 5. ANN model structure for the prediction of Hg^{2+} removal percentage.

4.3. Prediction results of ANN

The input variables of NNs significantly affect their efficiency, since they reflect the physical principles of the studied system. The input data have been

Table 1
Statistical parameters for ANN and ANFIS models

	ANN	ANFIS
R^2	0.997324526	0.996752844
SD	0.025438019	0.020938672
SSE	6.9395E−06	6.9395E−06
MSE	1.73488E−07	1.73488E−07
RMSE	0.000416518	0.000416518

normalized between zero and one prior to training step. The input variables in this study, as mentioned before, are initial pH of medium, temperature, and initial Hg^{2+} concentration. The structure of ANN in this study is illustrated in Fig. 5. As it can be seen, the network comprises three layers, including input, hidden, and the output. There are three nodes in input layer corresponded to three input operating variable. The inputs are directly sent from the input nodes to the hidden layer (considered one) by the weights, where the main data processing is performed there by the calculation of inputs weighted summation. The output layer has one node since there is only one output variable, Hg^{2+} removal percentage. It is worth noting that a set of initial values are assigned to weights which are corrected during the training through the comparison between experimental data and the model results. The minimization of errors is done as the result of their back propagation.

Seventy-five percent of all of experimental data are randomly selected for the training and the rest were used for the network testing. The hidden layer neuron number is determined through the minimization of difference between the validation set of data and the results of network calculations. LM algorithm presented more accurate results during the training compared with scaled conjugate gradient, gradient descent with momentum, adaptive learning rate back-propagation, and resilient back-propagation. Therefore, the current network was trained using LM algorithm. After the training, the network was tested by the new set of data which were not used during the training. Fig. 6 represents the graphical comparison between the experimental data and the results of ANN modeling. The value of correlation coefficient was 0.997, which denotes that the model output follows the target properly. It can be said that there is an excellent agreement between the experimental data and the results of modeling.

The standard deviation (SD) for the results of ANN modeling is equal to 0.025. The values of standard squared error (SSE), mean squared error (MSE), root-mean-square error (RMSE), R^2, and SD are reported in Table 1.

The high value of R^2 and the reported errors show that the output variations are shown well by the target. The results of modeling approved the fact that ANN is an appropriate tool to predict the performance of mercury bioremediation process.

Fig. 7 shows the evaluation of network error in training, validation, and testing as a function of learning epochs. The MSE became constant after 2 epochs which denotes the network convergence. Therefore, the acceptable error was achieved by 2 epochs.

4.4. Prediction results of ANFIS model

The structure of ANFIS model is illustrated in Fig. 8. Gaussian MF types were used during the current modeling study. The visual comparison between the experimental data and the results of ANFIS model has been shown in Fig. 9 with high value of $R^2 = 0.996$. This approves the high capability of ANFIS for the study of Hg^{2+} removal by the studied strain of PG02.

The deviation of predicted data by RSM, ANN, and ANFIS models from the Hg^{2+} removal percentage experimental data is illustrated in Fig. 10. The deviation intervals of RSM, ANN, and ANFIS predicted data are (−0.01296 to 0.013325), (−0.0192 to 0.03085), and (−0.02599 to 0.024057), respectively. Fig. 11 shows

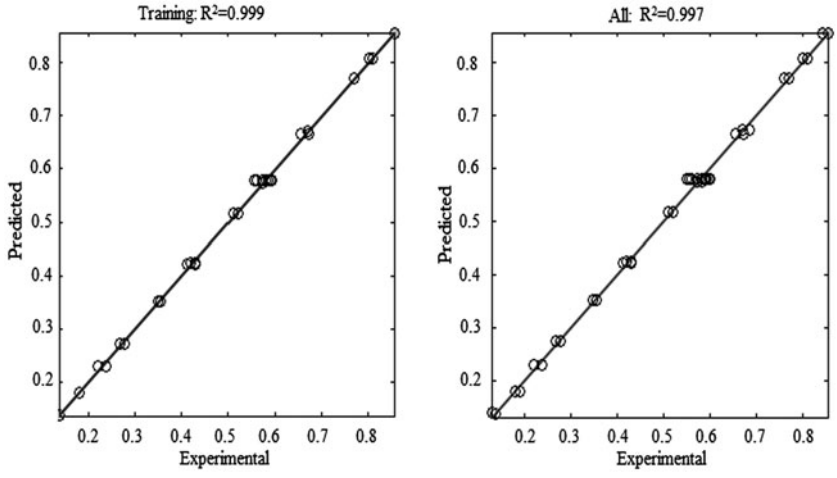

Fig. 6. Comparison of experimental data and predicted values by ANN for mercury removal by PG02.

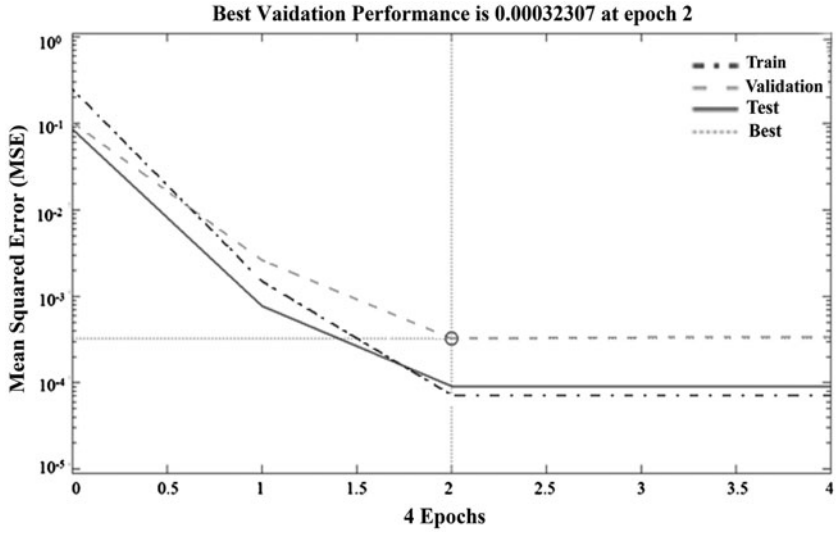

Fig. 7. Evolution of MSE values of training, validation, and test errors during ANN training.

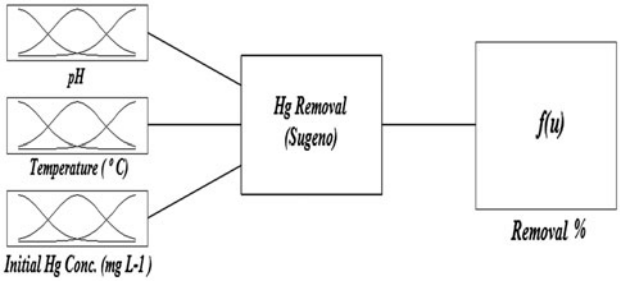

Fig. 8. The ANFIS structure for Hg^{2+} removal percentage modeling.

the comparison between the results of RSM, ANN, and ANFIS models and experimental data. There is an excellent agreement between the simulation results and the real data.

The results of ANN and ANFIS models can be compared with each other using Table 1 data through the reported figures for R^2, SD, SSE, and RMSE for two proposed models for prediction of Hg^{2+} removal percentage. These statistical parameters are calculated using Eqs. ((12)–(16)):

$$R^2 = \frac{\sum_{i=1}^{n}(Y_{\mathrm{Exp},i} - Y_{\mathrm{Model-Mean}})^2 - \sum_{i=1}^{n}(Y_{\mathrm{Model},i} - Y_{\mathrm{exp},i})^2}{\sum_{i=1}^{n}(Y_{\mathrm{Exp},i} - Y_{\mathrm{Model-Mean}})^2} \quad (12)$$

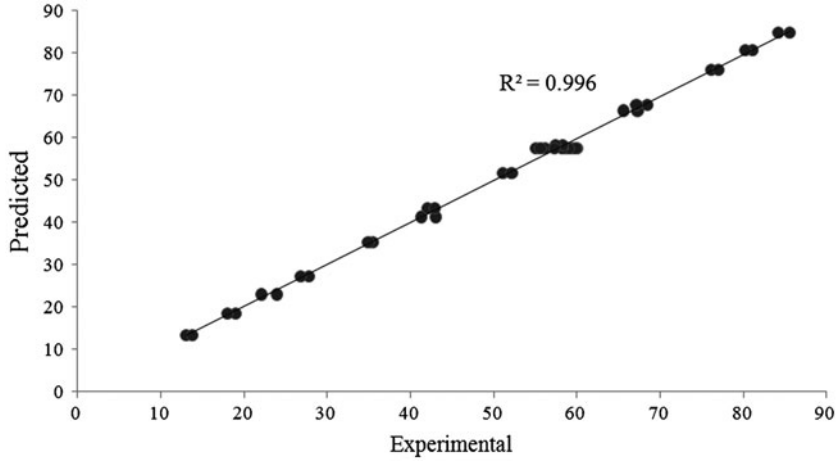

Fig. 9. Comparison of experimental data and predicted values by ANFIS for mercury removal by PG02.

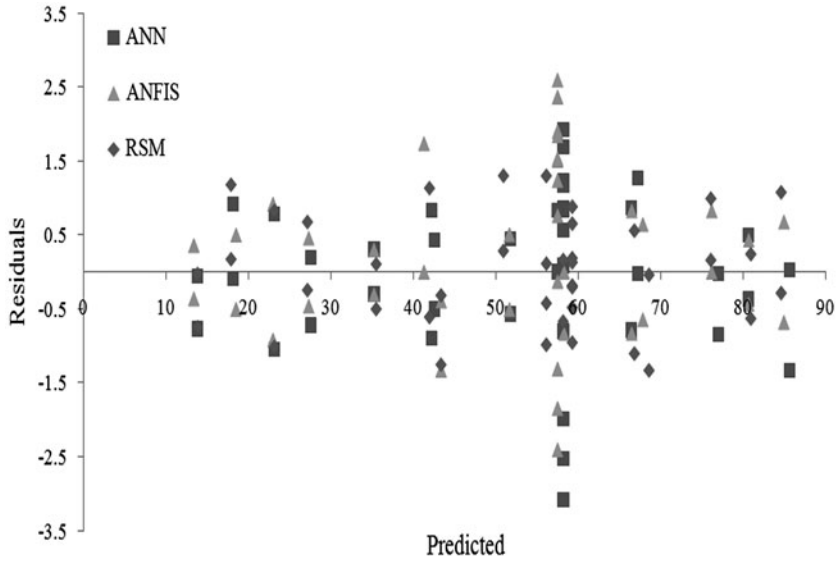

Fig. 10. The residuals vs. the predicted mercury removal percentage by ANN (■), ANFIS (▲), and RSM (♦).

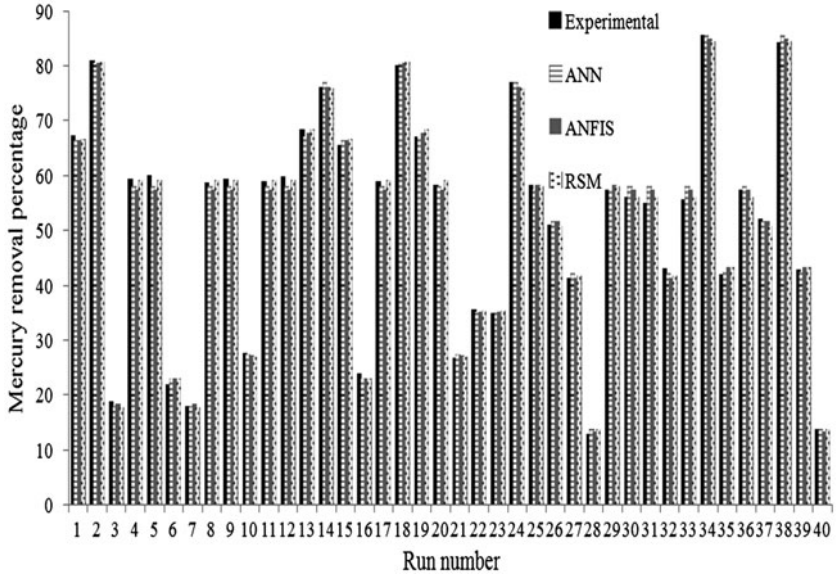

Fig. 11. Comparison of experimental mercury removal percentage and predicted values by ANN, ANFIS, and RSM in each run.

$$\mathrm{SD} = \sqrt{\frac{1}{n-1}\sum_{i=1}^{n}\left(\left|\frac{Y_{\mathrm{Exp},i} - Y_{\mathrm{Model},i}}{Y_{\mathrm{Exp},i}}\right| - \mathrm{AARE}\right)^2} \quad (13)$$

$$\mathrm{AARE} = \frac{1}{n}\sum_{i=1}^{n}\left(\left|\frac{Y_{\mathrm{Exp},i} - Y_{\mathrm{Model},i}}{Y_{\mathrm{Exp},i}}\right|\right) \quad (14)$$

$$\mathrm{SSE} = \sum_{i=1}^{n}\left(Y_{\mathrm{Model},i} - Y_{\mathrm{Exp},i}\right)^2 \quad (15)$$

$$\mathrm{RMSE} = \sqrt{\frac{\sum_{i=1}^{n}\left(Y_{\mathrm{Model},i} - Y_{\mathrm{Exp},i}\right)^2}{n}} \quad (16)$$

Table 2
The experimental and the predicted results of verification studies by RSM, ANN, and ANFIS under optimum conditions along with the corresponding percentage error values

	Studied factors				Predicted response along with percentage error					
Run	pH	Temp. (°C)	Initial Hg^{2+} Conc. (mg l^{-1})	Experiment[a] (%)	RSM (%)	Error (%)	ANN (%)	Error (%)	ANFIS (%)	Error (%)
1	7	37.5	5	93.08 ± 3.24	89	4.38	89.6	3.74	89.2	4.17
2	7	37.5	5	90.15 ± 2.69	89	1.28	89.6	0.61	89.2	1.05
3	7	37.5	5	91.46 ± 3.51	89	2.69	89.6	2.03	89.2	2.47
4	7	37.5	5	89.97 ± 1.36	89	1.08	89.6	0.41	89.2	0.86

[a]Values are mean ± SD, replicates = 2.

4.5. Verification tests

In order to approve the accuracy of the proposed models by RSM, ANN, and ANFIS approaches to predict mercury removal from aqueous solution by indigenous strain of *V. parahaemolyticus* PG02, four additional experiments were performed randomly under the optimum conditions which were achieved by Eq. (11). Table 2 shows the experimental results of the verification studies under the optimum factors along with the predicted values by RSM, ANN, and ANFIS models. Corresponding percentage errors have also been provided in order to compare the precisions.

As can be seen from Table 2, the maximum percentage error value for RSM results is 4.38%, while it is reported to be 3.74 and 4.17% for ANN and ANFIS, respectively. By taking the average of four percentage errors, it was found that the minimum obtained error value within the verification tests belonged to ANN model with the value of 1.70%, while the maximum value, 2.36%, obtained for RSM model. The small error values suggest significantly good predictions by the proposed models for mercury removal from aqueous solutions by the indigenous PG02 strain. However, the proposed ANN model was introduced as the best one.

5. Conclusions

Vibrio parahaemolyticus PG02, as an indigenous bacterial strain, can resist up to 45 mg l^{-1} mercury. The results showed that mercury removal ability by the strain decreased by increasing the mercury concentration in the medium. This was due to bacterial inactivation by their exposure to mercury. The investigations revealed that in the presence of initial 5 mg l^{-1} mercury, the PG02 survived for 40 h while simultaneously decreased the mercury concentrations in the medium. As the initial mercury concentration increased, the survival time decreased and consequently the rate of bioremediation decreased too. An experimental design strategy was performed by CCD under RSM in order to investigate the effect of studied factors on the response (mercury removal percentage) as well as evaluation of the proficiency of its modeling to predict the response. ANN and ANFIS were also established on the obtained experimental data to simulate the process and comparing their results. The high values of correlation of coefficients, R^2, revealed that each of these three approaches well fitted the experimental data and can be applicable for prediction of the process.

References

[1] C. Green-Ruiz, Mercury(II) removal from aqueous solutions by nonviable *Bacillus* sp. from a tropical estuary, Bioresour. Technol. 97 (2006) 1907–1911.
[2] H. Katırcıoğlu, B. Aslım, A.R. Rehber Türker, T. Atıcı, Y. Beyatlı, Removal of cadmium(II) ion from aqueous system by dry biomass, immobilized live and heat-inactivated *Oscillatoria* sp. H1 isolated from freshwater (Mogan Lake), Bioresour. Technol. 99 (2008) 4185–4191.
[3] E. Khoramzadeh, B. Nasernejad, R. Halladj, Mercury biosorption from aqueous solutions by sugarcane bagasse, J. Taiwan Inst. Chem. Eng. 44 (2013) 266–269.
[4] A. Sinha, S.K. Khare, Mercury bioremediation by mercury accumulating *Enterobacter* sp. cells and its alginate immobilized application, Biodegradation 23 (2012) 25–34.
[5] A. Sinha, K.K. Pant, S.K. Khare, Studies on mercury bioremediation by alginate immobilized mercury tolerant *Bacillus cereus* cells, Int. Biodeterior. Biodegrad. 71 (2012) 1–8.
[6] G. Bayramoğlu, M.Y. Arıca, Removal of heavy mercury(II), cadmium(II) and zinc(II) metal ions by live and heat inactivated Lentinus edodes pellets, Chem. Eng. J. 143 (2008) 133–140.
[7] R. Zhang, Y. Wang, J.D. Gu, Identification of environmental plasmid-bearing *Vibrio* species isolated from polluted and pristine marine reserves of Hong Kong, and resistance to antibiotics and mercury, Antonie van Leeuwenhoek 89 (2006) 307–315.

[8] A. Frischmuth, P. Weppen, W.D. Deckwer, Microbial transformation of mercury(II): I. Isolation of microbes and characterization of their transformation capabilities, J. Biotechnol. 29 (1993) 39–55.
[9] N. Sağlam, R. Say, A. Denizli, S. Patır, M.Y. Yakup Arıca, Biosorption of inorganic mercury and alkylmercury species on to *Phanerochaete chrysosporium* mycelium, Process Biochem. 34 (1999) 725–730.
[10] Y. Zeroual, A. Moutaouakkil, F.Z. Zohra Dzairi, M. Talbi, P.U. Ung Chung, K. Lee, M. Blaghen, Biosorption of mercury from aqueous solution by *Ulva lactuca* biomass, Bioresour. Technol. 90 (2003) 349–351.
[11] A. Cain, R. Vannela, L.K. Woo, Cyanobacteria as a biosorbent for mercuric ion, Bioresour. Technol. 99 (2008) 6578–6586.
[12] X.S. Wang, F.Y. Li, W. He, H.H. Miao, Hg(II) removal from aqueous solutions by *Bacillus subtilis* biomass, Clean 38 (2010) 44–48.
[13] M. Pepi, C. Gaggi, E. Bernardini, S. Focardi, A. Lobianco, M. Ruta, V. Nicolardi, M. Volterrani, S. Gasperini, G. Trinchera, Mercury-resistant bacterial strains *Pseudomonas* and *Psychrobacter* spp. isolated from sediments of Orbetello Lagoon (Italy) and their possible use in bioremediation processes, Int. Biodeterior. Biodegrad. 65 (2011) 85–91.
[14] J. Plaza, M. Viera, E. Donati, E. Guibal, Biosorption of mercury by *Macrocystis pyrifera* and *Undaria pinnatifida*: Influence of zinc, cadmium and nickel, J. Environ. Sci. 23 (2011) 1778–1786.
[15] H. Xie, Y.C. Lee, R.L. Mahajan, R. Su, Process optimization using a fuzzy logic response surface method, IEEE Trans. Compon. Packag. Manuf. Technol. Part A: 17(2) (1994) 202–211.
[16] O. Acaroglu, Prediction of thrust and torque requirements of TBMs with fuzzy logic models, Tunn. Undergr. Sp. Technol. 26(2) (2011) 267–275.
[17] M.A. Takassi, M.K. Salooki, M. Esfandyari, Fuzzy model prediction of Co (III)Al2O3 catalytic behavior in Fischer-Tropsch synthesis, J. Nat. Gas Chem. 20(6) (2011) 603–610.
[18] M. Chakraborty, C. Bhattacharya, S. Dutta, Studies on the applicability of artificial neural network (ANN) in emulsion liquid membranes, J. Membr. Sci. 220 (2003) 155–164.
[19] A. Meharrar, M. Tioursi, M. Hatti, A.B. Boudghène Stambouli, A variable speed wind generator maximum power tracking based on adaptative neuro-fuzzy inference system, Expert Syst. Appl. 38(6) (2011) 7659–7664.
[20] R. Abedini, M. Esfandyari, A. Nezhadmoghadam, B. Rahmanian, The prediction of undersaturated crude oil viscosity: An artificial neural network and fuzzy model approach, Pet. Sci. Technol. 30(19) (2012) 2008–2021.
[21] M. Balazinski, S. Achiche, L. Baron, M. Elektorowicz, A. El-Agroudy, Investigation of constructed wetlands efficiency in mercury removal using genetically generated fuzzy knowledge bases, 9th Canadian Society of Civil Engineering-Annual Conference, Ottawa, 2001.
[22] M. Elektorowicz, A. Qasaimeh, Fuzzy modeling estimation of mercury removal by wetland components, Fuzzy information-processing NAFIPS'04, Annual meeting of the IEEE, Alberta, 2004.
[23] B. Rahmanian, M. Pakizeh, M. Esfandyari, F. Heshmatnezhad, A. Maskooki, Fuzzy modeling and simulation for lead removal using micellar-enhanced ultrafiltration (MEUF), J. Hazard. Mater. 192 (2011) 585–592.
[24] B. Rahmanian, M. Pakizeh, S.A. Mansoori, Prediction of MEUF process performance using artificial neural networks and ANFIS approaches, J. Taiwan Inst. Chem. Eng. 43(4) (2012) 558–565.
[25] M. Shanbedi, D. Jafari, A. Amiri, S. Heris, M. Baniadam, Prediction of temperature performance of a two-phase closed thermosyphon using Artificial Neural Network, Heat Mass Transfer 49(1) (2013) 65–73.
[26] S. Aminossadati, A. Kargar, B. Ghasemi, Adaptive network-based fuzzy inference system analysis of mixed convection in a two-sided lid-driven cavity filled with a nanofluid, Int. J. Therm. Sci. 52 (2012) 102–111.
[27] D. Kim, S. Rhee, Design of an optimal fuzzy logic controller using response surface methodology, Fuzzy Syst. 9(3) (2001) 404–412. doi:10.1109/91.928737.
[28] R. Ravikumar, K. Renuka, V. Sindhu, K.B. Malarmathi, Response surface methodology and artificial neural network for modelling and optimization of distillery spent wash treatment using *Phormidium valderianum* BDU 140441, Pol. J. Environ. Stud. 22(4) (2013) 1143–1152.
[29] M.S. Mohamed, J.S. Tan, R. Mohamad, M. Noriznan Mokhtar, A.B. Ariff, Comparative analyses of response surface methodology and artificial neural network on medium optimization for *tetraselmis* sp. FTC209 grown under mixotrophic condition, Scientific World J. 2013 (2013) 14–28.
[30] M. Amini, H. Younesi, N. Bahramifar, A. Lorestani, F. Ghorbani, A. Daneshi, M. Sharifzadeh, Application of response surface methodology for optimization of lead biosorption in an aqueous solution by *Aspergillus niger*, J. Hazard. Mater. 154 (2008) 694–702.
[31] J.S. Kwak, Application of Taguchi and response surface methodologies for geometric error in surface grinding process, Int. J. Mach. Tools Manuf. 45(3) (2005) 327–334.
[32] D. Baş, İ.H. Boyacı, Modeling and optimization I: Usability of response surface methodology, J. Food Eng. 78(3) (2007) 836–845.
[33] M. Sarkar, P. Majumdar, Application of response surface methodology for optimization of heavy metal biosorption using surfactant modified chitosan bead, Chem. Eng. J. 175 (2007) 376–387.
[34] V.K. Devabhaktuni, M. Yagoub, Y. Fang, J. Xu, Q. Zhang, Neural networks for microwave modeling: Model development issues and nonlinear modeling techniques, Int. J. RF Microwave Comput. Aided Eng. 11(1) (2001) 4–21.
[35] I.K. Yilmaz, O. Kaynar, Multiple regression, ANN (RBF, MLP) and ANFIS models for prediction of swell potential of clayey soils, Expert Syst. Appl. 38(5) (2011) 5958–5966.
[36] J.S.R. Jang, ANFIS: Adaptive-network-based fuzzy inference system, IEEE Trans. Syst. Man Cybern. 23(3) (1993) 665–685. doi:10.1109/21.256541.
[37] H. Fazilat, M. Ghatarband, S. Mazinani, Z.A. Asadi, M.E. Shiri, M.R. Kalaee, Predicting the mechanical properties of glass fiber reinforced polymers via artificial neural

network and adaptive neuro-fuzzy inference system, Comput. Mater. Sci. 58 (2012) 31–37.
[38] H. Iyatomi, M. Hagiwara, Adaptive fuzzy inference neural network, Pattern Recognit. 37(10) (2004) 2049–2057.
[39] M. Mehrabi, S. Pesteei, T. Pashaee G., Modeling of heat transfer and fluid flow characteristics of helicoidal double-pipe heat exchangers using adaptive neuro-fuzzy inference system (ANFIS), Int. Commun. Heat Mass Transfer 38(4) (2011) 525–532.
[40] M.A. Shoorehdeli, M. Teshnehlab, A.K. Sedigh, Training ANFIS as an identifier with intelligent hybrid stable learning algorithm based on particle swarm optimization and extended Kalman filter, Fuzzy Sets Syst. 160(7) (2009) 922–948.
[41] S.A. Jafari, S. Cheraghi, M. Mirbakhsh, R. Mirza, A. Maryamabadi, Employing response surface methodology for optimization of mercury bioremediation by *Vibrio parahaemolyticus* PG02 in coastal sediments of Bushehr, Iran, CLEAN—Soil, Air, Water (in press). doi:10.1002/clen.201300616.
[42] J.H. Joo, S.H. Hassan, S.E. Oh, Comparative study of biosorption of Zn^{2+} by *Pseudomonas aeruginosa* and *Bacillus cereus*, Int. Biodeterior. Biodegrad. 64(8) (2010) 734–741.
[43] F. Kafilzadeh, N. Mirzaei, Growth pattern of Hg resistant bacteria isolated from Kor river in the presence of mercuric chloride, Pak. J. Biol. Sci. 11(18) (2008) 2243–2248.
[44] R.P.H. Schmitz, A. Eisenträger, W. Dott, Miniaturized kinetic growth inhibition assays with *Vibrio fischeri* and *Pseudomonas putida* (application, validation and comparison), J. Microbiol. Methods 31(3) (1998) 159–166.
[45] R. Zhang, Y. Wang, J.D. Gu, Identification of environmental plasmid-bearing *Vibrio* species isolated from polluted and pristine marine reserves of Hong Kong, and resistance to antibiotics and mercury, Antonie Van Leeuwenhoek 89 (2006) 307–315. doi:10.1007/s10482-005-9032-z.
[46] J. Walker, R. Colwell, Mercury-resistant bacteria and petroleum degradation, Appl. Microbiol. 27(1) (1974) 285–287.
[47] M. Kargar, M. Jahromi, M. Najafian, P. Khajeaian, R. Nahavandi, S. Jahromi, M. Firoozinia, Identification and molecular analysis of mercury resistant bacteria in Kor River, Iran, Afr. J. Biotechnol. 11(25) (2012) 6710–6717.
[48] I.E. Stas, B.P. Shipunov, I.N. Pautova, Y.V. Sankina, A study of adsorption of lead, cadmium, and zinc ions on the glass surface by stripping voltammetry, Russ. J. Appl. Chem. 77 (2004) 1487–1490. doi:10.1007/s11167-005-0057-x.
[49] M. Amini, H. Younesi, Biosorption of Cd(II), Ni(II) and Pb(II) from aqueous solution by dried biomass of *Aspergillus niger*: Application of response surface methodology to the optimization of process parameters, Clean 37(10) (2009) 776–786.
[50] M. Vidali, Bioremediation. An overview, Pure Appl. Chem. 73(7) (2001) 1163–1172.
[51] D. Guinot, R. Ureña, A. Pastor, I. Varó, J. Ramo, A. Torreblanca, Long-term effect of temperature on bioaccumulation of dietary metals and metallothionein induction in *Sparus aurata*, Chemosphere 87(11) (2012) 1215–1221.
[52] M. Odin, A. Feurtet-Mazel, F. Ribeyre, A. Boudou, Temperature, PH and photoperiod effects on mercury bioaccumulation by nymphs of the burrowing mayfly *hexagenia rigida*, in: Mercury as a Global Pollutant, Kluwer Academic Publishers, Springer, Whistler, 1995, pp. 1003–1006. doi:10.1007/978-94-011-0153-0_108